Research Article | Vol. 10, No. 8 / 1 August 2020 / Optical Materials Express 1962
Optical Materials EXPRESS

Photoluminescence and cathodoluminescence of $BaAl_2O_4:Eu^{2+}$ and undoped $BaAl_2O_4$: evidence for F-centres

DANIEL DEN ENGELSEN,[1] GEORGE R. FERN,[1] TERRY G. IRELAND,[1,*] FENGLI YANG,[1,2] AND JACK SILVER[1,*]

[1]Centre for Phosphor and Display Materials, Wolfson Centre for Materials Processing, Brunel University London, Uxbridge, Middlesex, UB8 3PH, UK
[2]School of Metallurgical Engineering, Jiangxi University of Science and Technology,Ganzhou 341000, China
*jack.silver@brunel.ac.uk

Abstract: In this article the photoluminescence (PL) and cathodoluminescence (CL) of undoped $BaAl_2O_4$ and $BaAl_2O_4$ doped with 500 ppm and 3 mol% Eu^{2+} is described. The most important results from the CL measurements are: (1) Undoped $BaAl_2O_4$ manifested intrinsic CL at 460 nm, which increased at low temperature and did not change significantly upon exposure to the e-beam; (2) Doping $BaAl_2O_4$ with Eu^{2+} changed the character of the intrinsic luminescence band: it became more sensitive to temperature variations and the band experienced a blue shift to ~425 nm; (3) electron beam (e-beam) exposure of $Ba_{0.97}Eu_{0.03}Al_2O_4$ at low temperature increased the 425 nm band strongly while the Eu^{2+} emission at ~500 nm decreased by about 70%. The Eu^{2+} emission band was symmetric, indicating that $BaAl_2O_4$:Eu has changed to the $P6_322$ phase upon e-beam exposure at low temperature; (4) We have identified the 460 nm band in undoped $BaAl_2O_4$ and the 425 nm band in $BaAl_2O_4:Eu^{2+}$ with F-centre luminescence, corresponding to the F-centre emission in α-Al_2O_3. The evidence for the assignment of the 425 nm band in $BaAl_2O_4:Eu^{2+}$ is the spectacular increase of the spectral radiance at 425 nm by e-beam exposure at 200 keV and low temperature. A preliminary model is presented that explains the results. The PL from $BaAl_2O_4:Eu^{2+}$ quenched at the rather low temperature of 140°C; this observation is explained in terms of thermal ionization of the Eu^{2+} ion.

1. Introduction

The late 1990s saw the advent of solid state "white" lighting in the market place. This was due to the production of white light from the combination of blue light from light emitting diodes (LEDs) with yellow light from a color converting emitting phosphor that was excited by part of the blue light from the LEDs [1,2]. Since then there has been continuous effort to find more efficient phosphors with emission bands in the visible part of the electromagnetic spectrum that could be used as colour converting materials in combination with either blue or near UV emitting diodes [1]. Such improved or new phosphors would find widespread use in both the lighting and display industries. In efforts to find such phosphors researchers have attempted to identify why some phosphor host lattices are better than others by trying to find relationships between structure, symmetry of the activator sites and the properties of the resulting emission bands (color, intensity and bandwidth). In the first generation of solid state "white" lighting, blue emitting LEDs were combined with the yellow emitting yttrium aluminium garnet doped with cerium (YAG:Ce). YAG:Ce is a very efficient phosphor and has been used by the solid state lighting industry as a yardstick comparison to evaluate the performance of new or improved phosphors. One of the

#377026 https://doi.org/10.1364/OME.10.001962
Journal © 2020 Received 4 Sep 2019; revised 28 Nov 2019; accepted 29 Nov 2019; published 27 Jul 2020

Optical Materials EXPRESS

problems of the combination blue LED + YAG:Ce is that an imperfect colour rendering index (CRI) results: too little red and green luminescence. Adding green and red emitting phosphors to the device can easily solve this problem, but then the lumen efficiency of the lamp worsens considerably [1–3]. In the last few years we have undertaken a systematic study of aluminate based phosphors to ascertain the properties of the phosphor and the host lattices. There are several compelling reasons to study the alkaline earth metal aluminate phosphors in addition to the obvious fact that they are related to YAG, these include their high stability, their ability to emit light in the blue (Ba- and Ca-aluminates) and the green (especially Sr-aluminates) regions of the visible spectrum, their widespread use as long afterglow phosphors and their rather low cost of fabrication.

Recently we have published the crystal structures of the phases found in the Eu^{2+} doped phosphor systems of $Sr_{1-x}Ca_xAl_2O_4$, $Ba_{1-x}Ca_xAl_2O_4$ and $Ba_{1-x}Sr_xAl_2O_4$ [4–6]. These studies were supported by analyses of the photoluminescence (PL) of these phosphor series and the cathodoluminescence spectra (CL) of the parent compounds $CaAl_2O_4$:Eu^{2+}, $SrAl_2O_4$:Eu^{2+} and $BaAl_2O_4$:Eu^{2+}. For $SrAl_2O_4$:Eu^{2+} a new hypothesis that explains the occurrence of the ~430 nm emission band at low temperature, viz. the presence of an F-centre was presented. Moreover, a new assignment of the deconvoluted components of the emission band of $CaAl_2O_4$:Eu^{2+} was put forward. In the case of $BaAl_2O_4$:Eu^{2+} it was found that by exchanging a small quantity of Ba for Sr, the hexagonal $P6_3$ structure (ferroelectric) changes to the more symmetric hexagonal $P6_322$ structure (paraelectric) [5]. This was a confirmation by spectroscopy of the work of Kawaguchi et al. [7], who discovered this phase transition by X-ray diffraction (XRD). The ferroelectric-paraelectric transition in pure $BaAl_2O_4$ was described earlier by various workers [8–11] based on X-ray diffraction (XRD), electron diffraction (ED) studies and analyses of the infrared spectrum. From these studies it was concluded that the ferroelectric-paraelectric phase transition in $BaAl_2O_4$ takes place between 400 and 450 K. In view of the extended investigations on the afterglow behaviour of $BaAl_2O_4$:Eu^{2+} co-doped with Dy^{3+} (see for example [12]), it is surprising that to date no study of the spectroscopic characteristics of this phase transition has been published.

The common assignment of the XRD-pattern of $BaAl_2O_4$ at room temperature to hexagonal $P6_3$ was criticised by Larsson et al. [13]. They claimed that the local structure of nano-domains in $BaAl_2O_4$ is most likely orthorhombic or monoclinic. This finding illustrates the fact that $BaAl_2O_4$ exists in various phases depending on temperature and synthesis conditions. Apart from the $P6_3 \rightarrow P6_322$ phase transition, there is another issue that makes $BaAl_2O_4$:Eu^{2+} interesting from a scientific point of view. The spectra of $BaAl_2O_4$:Eu^{2+} that have been published in the literature show unexplained differences: in some cases a shoulder or separate emission band at the low wavelength side (high energy side) of the main emission band appeared, whereas other workers did not find this shoulder or band. The situation regarding $BaAl_2O_4$:Eu^{2+} is summarised in Table 1, which is an extended version of the Table shown in Ref. [6]. The differences between the spectra in the literature are represented in Table 1 as the ratio r, which is the spectral radiance at about 430 nm divided by the spectral radiance at 500 nm. As mentioned in Ref. [6] it is impossible to identify one factor that is directly responsible for the different values of r in Table 1; however, it seems that the combination of adding a co-dopant and annealing at low temperature is maximizing r. Brito et al. [22] suggested that the origin of the band at 430 nm is due to the effect of water adsorption to the surface of the $BaAl_2O_4$ crystals. This hypothesis could not be verified by our analysis of the CL-spectrum of $BaAl_2O_4$:Eu that had a shelf life of about 3 years in air at room temperature [3], because that sample did not show a luminescence band at 430 nm.

An important factor that has not been indicated in Table 1 is the excitation condition, n. b. the current density or energy density of the exciting electron beam or radiation (UV or X-ray). This information is not available in the publications mentioned in Table 1, as it is usually considered to be irrelevant as long as saturation is not occurring.

Optical Materials EXPRESS

Table 1. Ratio between spectral radiances at 430 nm and 500 nm of $BaAl_2O_4:Eu^{2+}$.

r (ratio)	Spectrum	Annealing temp. (°C)	Annealing gas	co-dopant	Ref.
n. s.[a]	PL	≈1400	H_2/N_2	none	14
n. s.[a]	PL	1200	H_2/N_2	none	15
n. s.[a]	PL	1400	air/TCRA[b]	none	16
n. s.[a]	PL	1350	H_2/N_2	none	6
2.8	CL[c]	1350	H_2/N_2	none	5, 6
1.3	PL	500	combustion gases	Dy^{3+}	17
0.25	PL	550	combustion gases	none	18
0.05-0.5	PL	1500	air	Dy^{3+}	19
0.1	PL	1350	H_2/N_2	Dy^{3+}	20
0.8	CL	1200	H_2/N_2	none	21
0.15	PL (exc. 92 nm)	500	Combustion gases	Dy^{3+}	22
≈0.25	PL	≈1400	H_2/N_2	none	23

[a]n. s.: no shoulder or emission band at about 430 nm
[b]Thermal carbon reducing atmosphere.
[c]$Ba_{0.9}Sr_{0.07}Eu_{0.03}Al_2O_4$, measured at -170°C.

As mentioned above, $SrAl_2O_4$ doped with Eu^{2+} also shows a low-wavelength (high energy) emission band at 440 nm besides the main emission band at 520 nm at low temperature. Many investigations were carried out to determine the nature of this emission band [4,15,24–31]. There is no general agreement in the literature about the nature of this 440 nm emission band in $SrAl_2O_4:Eu^{2+}$, although the majority of authors agreed with Poort et al. [15] that the two emission bands in $SrAl_2O_4$ (monoclinic, space group $P2_1$) may be attributed to Eu^{2+} ions positioned at the two Sr sites that occur in equal amounts in the lattice. The problem with this assignment is that the asymmetry of the main band at 520 nm cannot be explained satisfactorily [4]. Bierwagen et al. [28] found that the 440 nm band in $SrAl_2O_4:Eu^{2+}$ increased strongly compared to the Eu^{2+} luminescence band at 520 nm upon decreasing the Eu concentration from 2% to 0.01%. They interpreted this result in terms of energy transport from one Eu^{2+} ion to another Eu^{2+} ion. An alternative explanation of their results is to assume that the 440 nm emission band is defect-based luminescence, which stays almost constant when varying the Eu concentration whereas the spectral radiance at 520 nm, being Eu^{2+} luminescence, is in line with the Eu concentration. In our work on $Sr_{1-x}Ca_xAl_2O_4:Eu^{2+}$ [4] we have elaborated on this alternative hypothesis and proposed that the origin of the 440 nm band in $SrAl_2O_4$ is due the luminescence of an F-centre. This proposal has been based on the work of Vitola et al. [32].

It was the objective of the work described herein to investigate whether the F-centre hypothesis could explain the 430 nm emission band in $BaAl_2O_4:Eu^{2+}$. In order to do so, we thought that including a study of the intrinsic luminescence of undoped $BaAl_2O_4$ could help to verify this hypothesis. Therefore we shall briefly review here the recent literature of the intrinsic luminescence of undoped $BaAl_2O_4$. Zhang et al. [33] measured the laser-activated (LA) spectra of undoped, reduced and non-reduced, $BaAl_2O_4$. The non-reduced $BaAl_2O_4$ did not show luminescence, while the samples reduced in H_2 at rather low temperatures of 700°C and 900°C produced a broad luminescence band at 750 nm. The sample that was doped with Eu^{2+} yielded also a broad emission band at 750 nm, which deviated strongly from our results [5,6] and those of other researchers indicated in our previous work. In contrast to the work of Zhang et al., both Pandey and Chithambo [34] and Benourdja et al. [35] reported a broad emission band at about 405 nm in the spectrum of undoped, non-reduced $BaAl_2O_4$. The first authors measured PL with UV-excitation at 248 nm and thermoluminescence, while the latter authors measured CL

Optical Materials EXPRESS

spectra. Both author groups attributed the broad emission band to native defect state transitions in $BaAl_2O_4$. Unlike Benourdja et al., Ayvacikli [36] did not observe CL upon exciting undoped $BaAl_2O_4$ with an e-beam of 25 keV, while Peng and Hong [16] could not measure any PL upon exciting undoped $BaAl_2O_4$ with UV-radiation at 340 nm. Finally, Suriyamurthi and Panigrahi [37] reported the PL at room temperature of undoped $BaAl_2O_4$ by excitation with near UV light at 346 nm. They recorded a main emission band at 500 nm and a shoulder at 430 nm and tentatively attribute these emission bands to V_k^{3+} defect centres. These contradictory results suggest that apart from the processes mentioned above, viz. annealing and excitation, there could be non-registered parameters such as synthesis conditions (e.g. grinding), purity (e.g. rare earth contamination), storage condition (e.g. humidity), etc. that affect the nature and concentration of defects in $BaAl_2O_4$.

2. Experimental

2.1. Sample definition and synthesis conditions

Table 2 presents the samples that were investigated in the current study.

Table 2. Sample definition of doped and undoped $BaAl_2O_4$.

Sample	Eu concentration (molar fraction)	Final annealing conditions
BA1	<5ppm	60 hrs. in air at 950°C
BA2	<5ppm	as BA1 + 24 hrs. in H_2/N_2 at 950°C
BA3	500 ppm	2 hrs. in H_2/N_2 at 1350°C
BA4	500 ppm	as BA3 + 2 hrs. in air at 1350°C
BA5	3%	2 hrs. in H_2/N_2 at 1350°C

Starting materials were: barium carbonate (Alfa Aesar, UK, 99%), aluminum oxide (SASOL Inc., USA), europium oxide (Ampere Industrie, France, 99.99%), and concentrated hydrochloric acid (Sigma Aldrich, UK, 37%), H_2/N_2 mixed gas with about 5% H_2. All materials were used as supplied without further purification. BA5 ($Ba_{0.97}Eu_{0.03}Al_2O_4$) was prepared by calcining mixtures of an appropriate molar ratio of $BaCO_3$, γ-Al_2O_3 and $EuCl_3$ powders in a flow of 90% N_2–10% H_2. After calcination the powder was ground by ball milling (Al_2O_3) for 3 hours. The final annealing was at 1350°C under H_2/N_2 for 2 hours. Sample BA3 was made using the same procedures. From an analysis of the Raman spectra of the samples BA5 and BA3 it was concluded that the latter sample contained 500 ± 100 ppm Eu. Sample BA1, $BaAl_2O_4$ without a detectable Eu concentration (by Raman spectroscopy using the 532.1 nm emission of a YAG-Nd laser and (separately) the 632.8 nm emission of a He-Ne laser), was obtained from ABCR (Karlsruhe, Germany). By X-ray diffraction (XRD) it was determined that ABCŔs material had partly been decomposed into $BaCO_3$ and Al_2O_3 due to prolonged shelf life in air. Before recording any CL spectra, this material was annealed for 60 hours at 950°C in air; after this treatment it was determined by XRD that the material had the hexagonal $P6_3$ structure of $BaAl_2O_4$ (~100%).

2.2. Characterisation and spectroscopy

The crystallinity of the samples listed in Table 2 was verified by X-ray powder diffraction using a Bruker D8 Advance X-ray diffractometer fitted with a nickel-filtered copper source, CuKα at λ=1.5406 Å, and a LynxEye silicon strip detector [4].

These samples were also investigated in a transmission electron microscope (TEM), (2100F, JEOL, Japan) equipped with a Schottky-type field emission gun. The TEM was equipped with a Vulcan cathodoluminescence (CL) detector, Gatan, USA, for imaging and spectroscopic purposes. This system used a Czerny–Turner spectrometer with back-illuminated CCD and gratings with 1200 or 2400 grooves per mm for collection of the CL spectra. The wavelength range of this

Optical Materials EXPRESS

spectrometer was from 380 nm to 900 nm. A small cryostat connected to the sample holder enabled cooling of the samples in the TEM down to 103 K (-170°C); adjustment of the sample temperature to any value between 103 K and 303 K could be made.

CL spectra of $BaAl_2O_4$:Eu^{2+} were recorded with the Gatan spectrometer in TEM- and rarely in STEM-mode. The relevant difference between these modes is the defocussed e-beam in TEM-mode, whereas in STEM-mode the e-beam is focussed. In the TEM-mode the current density j depends on the magnification. In our experiments it was $0.001 < j < 0.01$ A/cm^2, whereas in STEM-mode and a non-scanning or stationary e-beam it was several orders of magnitude larger. The high current density in stationary STEM-mode yielded (sometimes) non-reproducible results, probably due to some heating of the sample; therefore, this mode was only used in a few cases for checking purposes.

PL excitation and emission spectra of the samples were recorded using a Bentham phosphor spectrometer system (Bentham Instruments Ltd., Reading, UK.), configured with M300 excitation and emission monochromators, which were equipped with 0.2 mm slits. The absolute wavelength calibration of this emission monochromator had maximal error of 0.4 nm.

Laser-induced fluorescence spectra of the samples defined in Table 2 were measured with a Horiba Jobin Yvon Labram HR monochromator by excitation with a YAG-Nd laser (second harmonics at 532.1 nm) at room temperature. These measurements were done to check the Eu doping concentration of the samples defined in Table 2. The laser-Raman measurements of these materials are described in detail in a separate paper [38] and will not be described herein. The method to determine the Eu concentration is based on the ratio between the spectral radiances of the strong Eu^{3+} $^5D_0 \rightarrow {}^7F_2$ transition and the lattice vibration of $BaAl_2O_4$ at a Raman Shift of 243 cm^{-1}. The spectral radiance of this lattice vibration is assumed not to change as a function of the Eu doping, while the BA5 sample with 3% Eu has been adopted as the calibration sample. From these measurements the Eu concentration in the other samples has been checked.

3. Results

3.1. Morphology and structure

Figures 1(a), 1(b) and 1(c) present electron microscope images of BA5 crystals. Figure 1(a) is a TEM-image, while Figs. 1(b) and 1(c) are a high-angle annular dark-field (HAADF) and pan chromatic image respectively of the same area. The size of the particles in this sample varied between about 0.5 µm to about 5 µm. For the CL measurements we used particles with a diameter > 1 µm. Figure 1(d) is a TEM-image that was recorded of BA1 (ABCŔs undoped $BaAl_2O_4$ after 60 hrs. annealing in air at 950°C).

From the XRD patterns recorded at room temperature it was concluded that all samples presented in Table 2 consisted of one phase, namely the hexagonal $P6_3$ structure (ferroelectric) [5,6].

3.2. Photoluminescence and cathodoluminescence

Figure 2 presents the CL spectra of undoped $BaAl_2O_4$ (BA1) that was annealed in air. By reducing this sample we got sample BA2, which yielded CL spectra that were very similar to the spectra presented in Fig. 2. So, the occurrence of intrinsic luminescence in $BaAl_2O_4$ does not depend critically on the annealing conditions when high energy electrons are used for the CL measurements.

Figure 2 indicates that BA1 has a rather strong intrinsic luminescence when hit by an e-beam of 200 keV. The emission peak is at about 465 nm and it manifests a small blue shift upon lowering the temperature. The spectral radiance has a tendency to increase upon lowering the temperature. The spread in the spectral readiance is substantial: this is caused by the manual positioning of the e-beam on the same crystal cluster. The spectra shown in Fig. 2 manifested no significant changes

Optical Materials EXPRESS

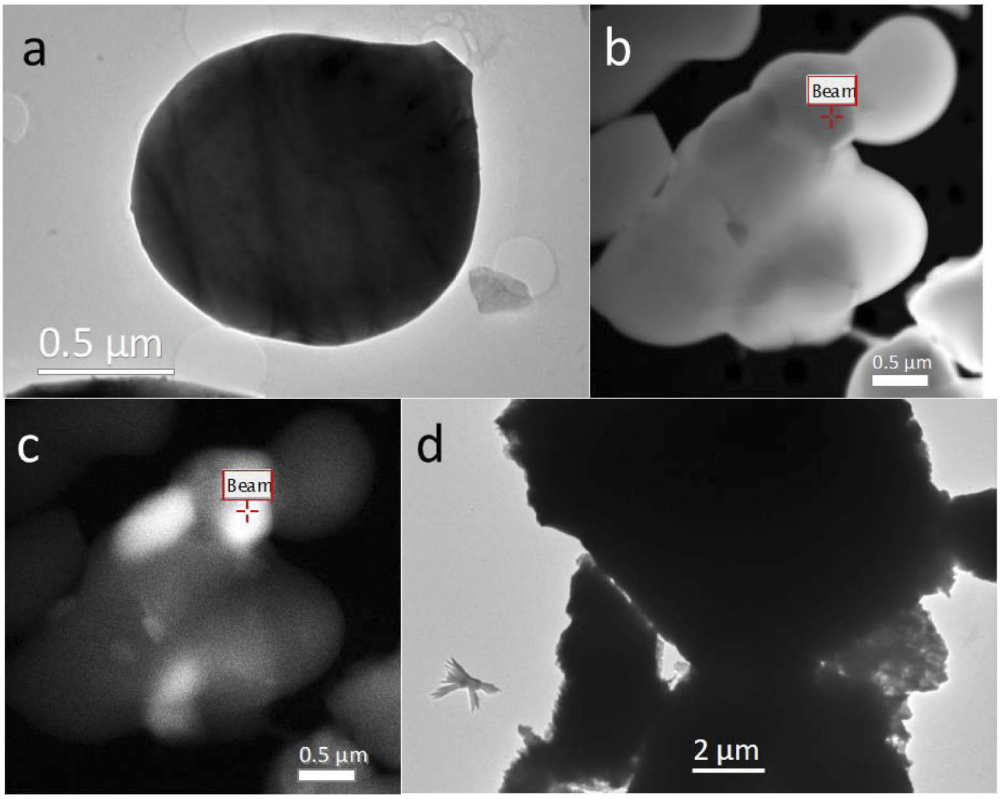

Fig. 1. TEM and STEM images recorded at 200 keV and -169°C. (a) TEM image of BA5 ($Ba_{0.97}Eu_{0.03}Al_2O_4$). (b) HAADF image of BA5. (c) Pan chomatic image of the same area shown in b."Beam" indicates a position, where the crystal was hit by the e-beam for some time before measuring the CL spectrum (in STEM mode). (d) TEM image of BA1 (ABCR's undoped $BaAl_2O_4$ after annealing for 60 hrs. in air).

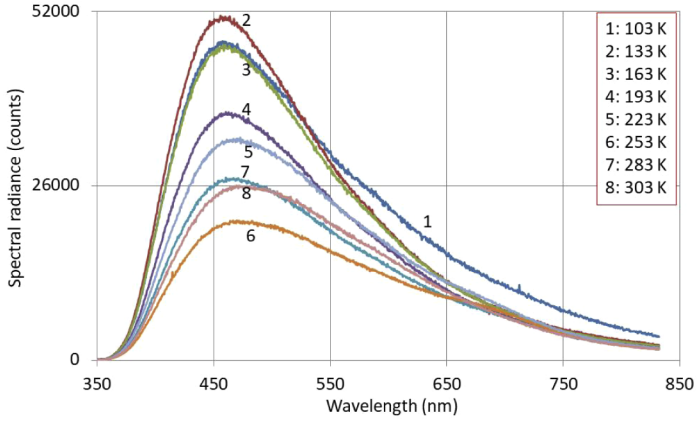

Fig. 2. CL spectra of BA1 (undoped $BaAl_2O_4$ annealed at 950°C in air for 60 hrs). The spectra were recorded from the same crystal cluster in TEM-mode. Thermal drift was corrected manually: this caused some spread in the spectral radiance.

Optical Materials EXPRESS

to those obtained from other crystals when they were exposed to the e-beam. That means that the orientation of the hexagonal crystal upon excitation is not an important parameter. Figure 3 presents a deconvolution of the -169.9°C spectrum of Fig. 2.

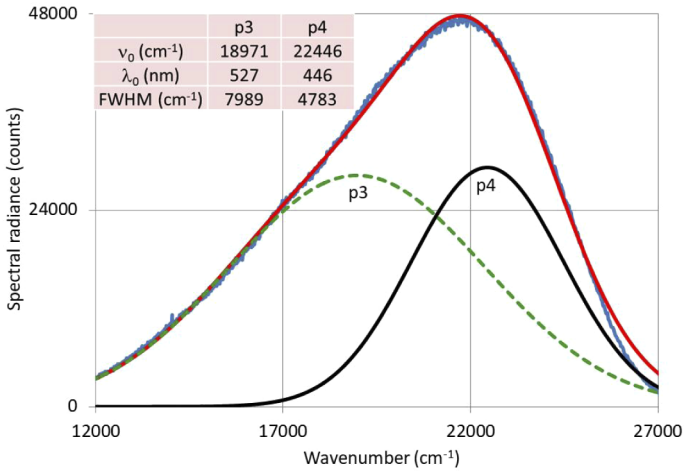

Fig. 3. Deconvolution of 103 K spectrum of Fig. 2. The spectrum can be well represented by two Gaussian profiles in a wavenumber base. The insert indicates the peak wavenumber (ν_0), peak wavelength (λ_0) and full width at half maximum (FWHM) of the two profiles p3 and p4.

The deconvolution of spectra with Gaussian profiles has been described in detail in our previous work [4–6]. As mentioned in section 2.2, the rather steep slope of the spectral radiance between 360 nm and 400 nm in Fig. 2 is partially caused by the cut-off wavelength of the detector of the spectrometer. It might well be that the intrinsic emission band of undoped $BaAl_2O_4$ is extending further into the near UV than indicated in Fig. 2. If that is the case, then λ_0 of the p4 profile will slightly shift to the blue.

In the introduction we have mentioned some recent studies on the intrinsic luminescence of undoped $BaAl_2O_4$ [33–37] and undoped $SrAl_2O_4$ [32]. Since the published spectra of undoped $BaAl_2O_4$ show substantial differences, there is no obvious way to select an appropriate spectrum for comparison. The PL spectrum of undoped $BaAl_2O_4$ reported by Suriyamurthi and Panigrahi [37] comes closest to the result presented in Fig. 3. Their main band at ~490 nm could be compared with λ_0 at 527 nm of p3 and their shoulder at 440 nm with λ_0 at 446 nm of p4. A big difference between Fig. 3 and the spectrum of Suriyamurthi and Panigrahi is the width of the emission band, which is much larger for the CL spectrum in Fig. 3. The agreement between Fig. 3, which refers to undoped $BaAl_2O_4$, and the spectrum of undoped $SrAl_2O_4$ at low temperature [32] is surprisingly good, taking into account the preliminary character of the deconvolution presented in Fig. 3. Vitola et al. [32] assigned the 435 nm band in undoped $SrAl_2O_4$ to an F-centre and the 510 nm band to an F_2-centre. The luminescence of these defects in α-Al_2O_3 and γ-Al_2O_3 has been well described in the literature [39–46] and as mentioned by Vitola et al. [32], the wavelength of the luminescence peaks does not depend strongly on the crystal structure, α- or γ-Al_2O_3. This was confirmed by Zorenko et al. [44], who determined λ_0 of the F-centre luminescence in YAG at 464 nm and in YAP at 423 nm. Based on the similarity of the F-centre luminescence in Al_2O_3 and the mentioned aluminates, we assume that the 446 nm profile (p4) in undoped $BaAl_2O_4$ may be attributed to an F-centre. This assumption will be elaborated in more detail in the discussion section. Assigning the 527 nm profile of Fig. 3 to an F_2-centre seems to be unlikely because, as indicated by Itou et al. [41], the generation of F_2–centres in α-Al_2O_3

Optical Materials EXPRESS

requires annealing at high temperature in a strongly reducing atmosphere or bombarding with a high flux of neutrons. An alternative assumption is that p3 represents the luminescence from an F-centre that is located at a different oxygen vacancy, which is the origin of F-centre emission bands in aluminates. According to this idea both p3 and p4 are due to different F-centre emission bands.

Figure 4 presents CL spectra of sample BA3 ($BaAl_2O_4$ with 500 ppm Eu) recorded at various temperatures and 200 keV.

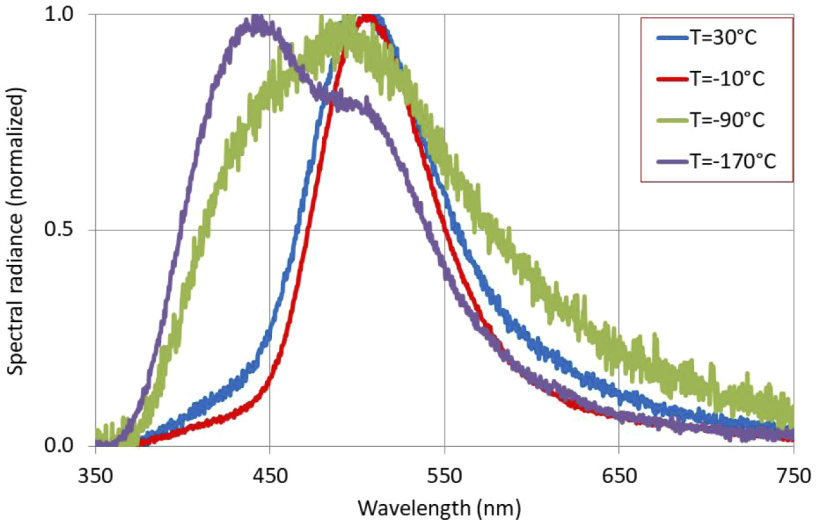

Fig. 4. CL spectra of BA3 ($BaAl_2O_4$ with 500 ppm Eu) recorded in TEM-mode at 200 keV and various temperatures. The spectral radiance at -90°C was low (likely due to slightly wrong positioning of the e-beam): for better comparison the ordinate has been normalised.

In the spectrum of BA3 recorded at -170°C presented in Fig. 4 two emission bands can clearly be observed: one at ~440 nm and the other at 500 nm. The high temperature band at 500 nm may be ascribed to the 5d→4f transitions of Eu^{2+} in $BaAl_2O_4$, whereas it is obvious to identify the low temperature 440 nm band with the high-energy intrinsic emission band (p4) of $BaAl_2O_4$ presented in Fig. 3. The two emission bands in the -170°C temperature spectrum of Fig. 4 match perfectly with the emission bands of undoped $BaAl_2O_4$ published by Suriyamurthi and Panigrahi [37]. So, the question arises whether the 500 nm band recorded by Suriyamurthi and Panigrahi should be assigned to Eu^{2+}. Anyhow, the close correspondence between the spectra shown in Fig. 4 on the one hand and those shown in Figs. 2 and 3 on the other hand indicates how important it is to study undoped $BaAl_2O_4$ that has no (detectable) Eu contamination.

Figure 5 presents the PL and CL spectra of BA5 ($BaAl_2O_4$:3%Eu^{2+}) at 25°C.

The Eu^{2+} emission bands shown in Fig. 5 are also asymmetric and cannot be represented by one Gaussian profile, but rather need two Gaussian profiles. In hexagonal ($P6_3$) $BaAl_2O_4$ there are two different Ba sites in a ratio 1:3 [14,47]. Poort et al. [14] confirmed from luminescence decay measurements that the emission band of $BaAl_2O_4$:Eu^{2+} consisted of two separate emission centres. The ratio Rp1/Rp2 of the radiances (integrated intensities) of the two profiles in Figs. 5(a) and 5(b) is 0.77 and 0.44 for the PL and CL spectrum respectively, which is larger than the ratio Ba(1)/Ba(2) for hexagonal $P6_3$ $BaAl_2O_4$. This result could indicate that the energy transport to the Eu^{2+} ion postioned at Ba(1) is larger than the transport to the Eu^{2+}ion at Ba(2) if the ratio Eu^{2+}(1)/Eu^{2+}(2) is equal to Ba(1)/Ba(2), which is commonly assumed. However, there are more factors that may affect the ratio Rp1/Rp2: one refers to the the excitation conditions and a second

Optical Materials EXPRESS

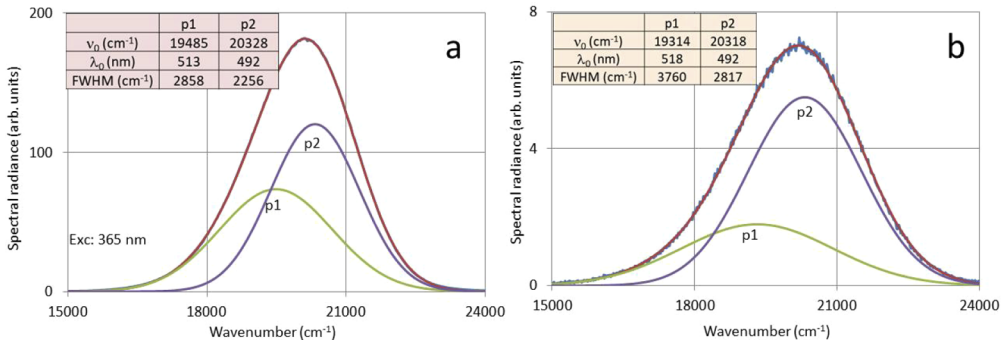

Fig. 5. PL (a) and CL (b) spectra of $Ba_{0.97}Eu_{0.03}Al_2O_4$ (BA5) at room temperature. The CL spectrum was recorded with the Gatan spectrometer at 200 keV. For deconvolution, see legend of Fig. 3. The profile indications p1 and p2 have been reserved for the Eu^{2+} emission band.

to the different crystal fields at the two Ba sites. Furthermore, we assume it to be unlikely that any quenching occurs at the Eu^{2+} concentrations used.

In Fig. 6 the PL spectra of $BaAl_2O_4:Eu^{2+}$ between 25°C and 125°C have been plotted.

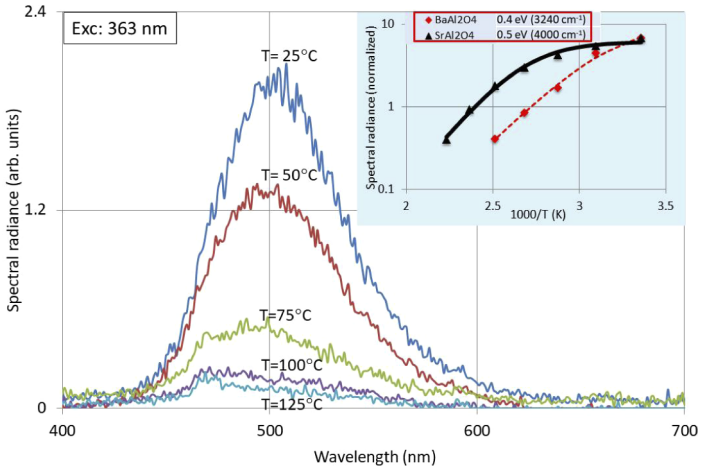

Fig. 6. PL spectra of $BaAl_2O_4:Eu^{2+}$ (Exc. 363 nm) recorded at various temperatures. The insert shows an Arrhenius analysis of the maximal spectral radiances of $BaAl_2O_4:Eu^{2+}$ and $SrAl_2O_4:Eu^{2+}$ (both with 3 mol% Eu^{2+}). The curves were fitted to the experimental points with the Fermi-Dirac equation.

It can be seen that the PL is quenched at a temperature of ≈140°C, which agrees with the finding of Poort et al. [14] who found the quenching temperature (T_q) of this phosphor at 137°C, whereas Lizzo et al. [48] reported a quenching temperature of 205°C. The spectrum at 25°C in Fig. 6 is noisier than the spectrum shown in Fig. 5(a), because different monochromators (and detectors) were used for the recordings. We also measured the quenching behaviour of $SrAl_2O_4:Eu^{2+}$ and found T_q=195°C, which is lower than 280°C reported by Poort et al. [14] and 205°C reported by Lizzo et al. [48], but considerably higher than the T_q of $BaAl_2O_4:Eu^{2+}$. In Fig. 6 an Arrhenius plot of the maximum radiances of $BaAl_2O_4:Eu^{2+}$ and $SrAl_2O_4:Eu^{2+}$ has been inserted. As described in our previous work on the LA-spectra of $Y_2O_3:Er^{3+}$ [49], the thermal quenching of luminescence in phophors can be represented by the Fermi-Dirac equation

Optical Materials EXPRESS

with one barrier energy E_q:

$$SR(T) = \frac{C}{1 + Be^{-E_q/kT}}, \quad (1)$$

where C and B are constants to be fitted, k is Boltzmann's constant and T is the absolute temperature. The barrier energies for $BaAl_2O_4$:Eu^2 and $SrAl_2O_4$:Eu^{2+} are found to be 0.4 ± 0.2 eV and 0.5 ± 0.2 eV respectively. The emission bands presented in Fig. 6 are asymmetric: this is to be expected for the $P6_3$ phase with two different Ba sites, where two Eu^{2+} ions can be located. At temperatures >130°C the change to the more symmetric $P6_322$ phase with one Ba site is to be expected. By adding a small quantity of Sr to $BaAl_2O_4$:Eu^{2+} we have observed this phase change at room temperature [5], as mentioned in the introduction. In the discussion section the quenching behaviour shown in Fig. 6 will be explained in terms of thermal ionization of Eu^{2+} by electron transfer to the conduction band of $BaAl_2O_4$.

Figure 7 presents CL spectra recorded at -169.8°C after varying the periods of bombarding a $Ba_{0.97}Eu_{0.03}Al_2O_4$ (BA5) crystal with electrons in the TEM at 200 keV.

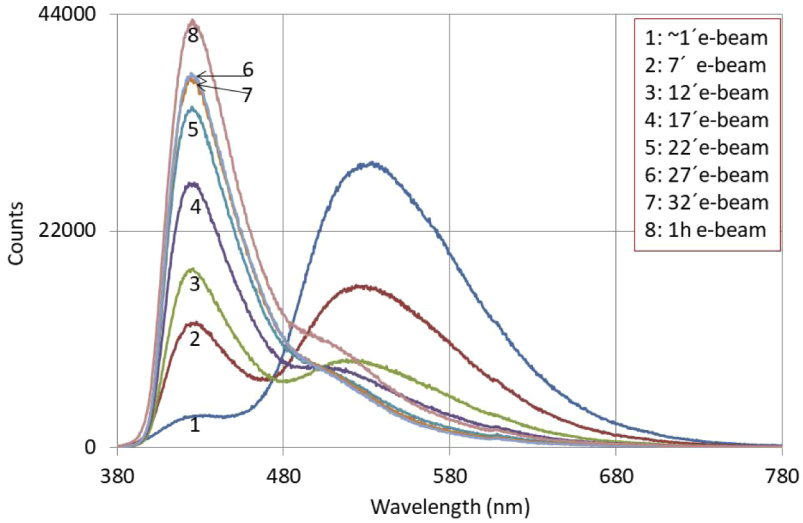

Fig. 7. CL spectra of BA5 recorded at -169.8°C and 200 keV. The eight spectra were recorded after various time periods (from 1 minute to 1 hour) of bombarding the specimen in TEM-mode with a current density of about 7 mA/cm^2.

Figure 7 illustrates that exposure of a crystal cluster of $BaAl_2O_4$:Eu^{2+} to an electron beam (e-beam) at low temperature induced major changes in the spectrum. It was found that bombarding $BaAl_2O_4$:Eu^{2+} with electrons at 25°C did not lead to any spectral change; hence, the first condition for the spectral change observed in Fig. 7 is the need for low temperature. The second condition is the exposure time to the e-beam. Longer exposure times led to an increase of the band at ~425 nm and decrease of the luminescence at ~510 nm. It was impossible to measure a spectrum of a crystal immediately after the e-beam hit it, because some time was needed for adjusting the e-beam and focussing it. By extrapolating the trend of Fig. 7 to 0 minutes it can be estimated that the main emission band of $BaAl_2O_4$:Eu^{2+} experienced a red shift of about 25 nm on cooling down from 25°C to -169.8°C. After 1 hour of e-beam exposure no further significant changes were observed. This finding was confirmed by exposing some sites to much higher current densities in STEM-mode with a stationary beam. In this case only the end stages, i.e. the spectra 5-8 in Fig. 7, could be observed, because the changes occurred too fast with the consequence that the early stages (i.e. spectra 1-4 in Fig. 7) could not be measured. So, the spectra 6-8 in Fig. 7 refer to the (almost) "fully converted" situation. It should be noted that spectra 1-3 of

Optical Materials EXPRESS

Fig. 7 show an isosbestic point demonstrating that only two component peaks are involved in the initial change; that is a broad band is growing in intensity as another is losing intensity The fact that spectra 4-8 in Fig. 7 deviate from the isosbestic point indicates that the two sites in the spectra that were fitted by the two Gausians in Fig. 5 (p1 and p2) change at different rates with time in the e-beam with p1 lasting longer. In spectra 4-8 it can be seen that the emission band at ~430 nm grows as a function of time; this feature will also be disscussed below. In spectrum #8 of Fig. 7 the ratio between the spectral radiances at λ=425 nm and at λ=500 nm is 3.9. E-beam exposure at -170°C on other crystals at a lower current density resulted in a lower ratio between the mentioned spectral radiances; however, the effect of current density on the spectral change has not been studied quantitatively in this work. Nevertheless, we made some observations using a focussed and stationary beam in STEM-mode with a much higher current density. In this case the changes shown in Fig. 7 occurred in a few minutes. However, since this caused some beam damage, no quantitative data were collected. Returning to the discussion on the presence of the isosbestic piont for spectra 1-2 of Fig. 7 it can be seen (in Fig. 9) that initially both components p1 and p2 of the ~510 nm band initially decrease at the same rate. However, in the succeeding spectra 3-8 p1 and p2 change at different rates (p1 dissappears completely) and so the isobestic piont is not retained. This is additional evidence that the 500 nm band is made up of two bands as we have fitted it in this work.

At a temperature of -170°C after prolonged e-beam exposure the crystal used for the experiment presented in Fig. 7 remained in the converted state for hours. After warming up the sample, the original spectrum before cooling down and e-beam exposure returned. In other words, the process depicted in Fig. 7 is reversible. Although the 425 nm band in the spectra 2-8 of Fig. 7 is positioned at a lower wavelength than than the intrinsic emission bands of $BaAl_2O_4$ in Fig. 2, it is assumed that this band may be assigned to luminescence from defect states of $BaAl_2O_4$, notably emission from the F-centre. An argument in favour of this assumption is the increase of the 425 nm band by e-beam exposure (at low temperature). Bombarding α-Al_2O_3 by neutrons and electrons is a well known technique to activate the F-centre luminescence in this material [41–46]. We expect that this is also the case in $BaAl_2O_4$:Eu^{2+}.

The F-centre band in BA3 (with 500 ppm Eu) has an intermediate position as illustrated in Fig. 8. The remarkable results listed in Table 1 about the occurrence of the 425-430 nm band in the spectrum of $BaAl_2O_4$:Eu^{2+} can now be understood with this hypothesis. We assume that the concentration of F-centres in $BaAl_2O_4$ behave more or less identical to the F-centres in α-Al_2O_3; i.e., it depends on the preparation conditions, such as annealing temperature and gas atmosphere (reducing versus oxidising), and the excitation conditions such as radiation intensity and energy (PL) and current density and energy (CL).

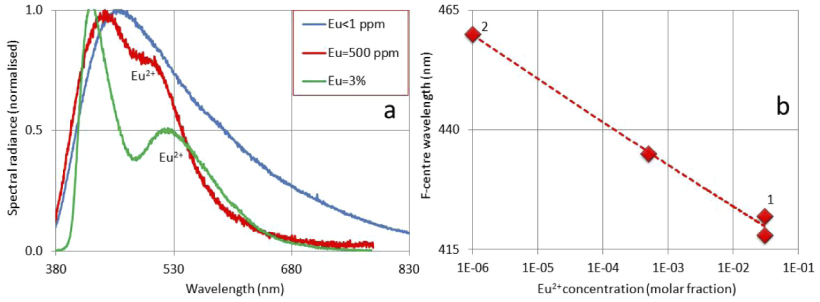

Fig. 8. (a): Comparison of CL spectra of $BaAl_2O_4$ with various Eu concentrations recorded at -170°C. (b): F-centre wavelength in $BaAl_2O_4$:Eu^{2+} versus Eu molar fraction. 1 = $Ba_{0.9}Sr_{0.07}Eu_{0.03}Al_2O_4$, 2 = BA1 (undoped $BaAl_2O_4$), which is assumed to have a Eu^{2+} concentration of ~1 ppm. The dashed line has been fitted through the experimental points.

Optical Materials EXPRESS

Figure 8 indicates that the F-centre band manifests a blue shift when the Eu^{2+} concentration is increased in $BaAl_2O_4$. It should be mentioned that the peak wavelengths of the non-deconvoluted bands have been indicated in Fig. 8(b). The presented blue shift of the maximum wavelength of the F-centre in Fig. 8 implies that we are likely dealing with an interaction between the F-centre and the inserted Eu ion. We are currently studying this interaction in a number of aluminate structures and we intend to publish more about this phenomenon in the near future.

In Fig. 9 the results of deconvolutions of CL-spectra of $BaAl_2O_4$:Eu at -170°C are presented. This deconvolution analysis indicates that the Eu^{2+} emission band of $BaAl_2O_4$:Eu^{2+} at 18825 cm^{-1} (531 nm) after only 1 minute e-beam exposure must be represented by two Gaussian profiles in Fig. 9(a), while after >12 minutes e-beam exposure only one Gaussian profile is sufficient, as indicated in Figs. 9(b) and 9(c). Simultaneously the radiance of the Eu^{2+} emission band is decreasing while the F-centre emission band, consisting of two Gaussian profiles (p3 and p4), at 23630 cm^{-1} (423 nm) is growing. As mentioned above, the two profiles of the Eu^{2+} band after a short-time e-beam exposure may be assigned to the emission of two Eu^{2+} ions located at the two different Ba sites in the $P6_3$ ferroelectric phase of $BaAl_2O_4$. After prolonged e-beam exposure the Eu^{2+} emission band becomes symmetric indicating that $BaAl_2O_4$ has been transferred to the $P6_322$ paraelectric phase with only one unique Ba site.

Finally, the deconvoluted Cl-specrum of BA3 in Fig. 9(d) indicates that the Eu^{2+} emission band is almost symmetric, because the radiance of the p1 profile is small compared to the radiance of p2. In other words, the transtion from the ferroelectric to the paraelectric phase of $BaAl_2O_4$ has not yet completed at low Eu^{2+} concentration. By comparing Fig. 9(a) with Fig. 5 it can be seen that the ratio of the radiance of the profiles p1 and p2 has changed considerably. The spectra of Fig. 5 were recorded at room temperaure: it is assumed that the F-centre emission

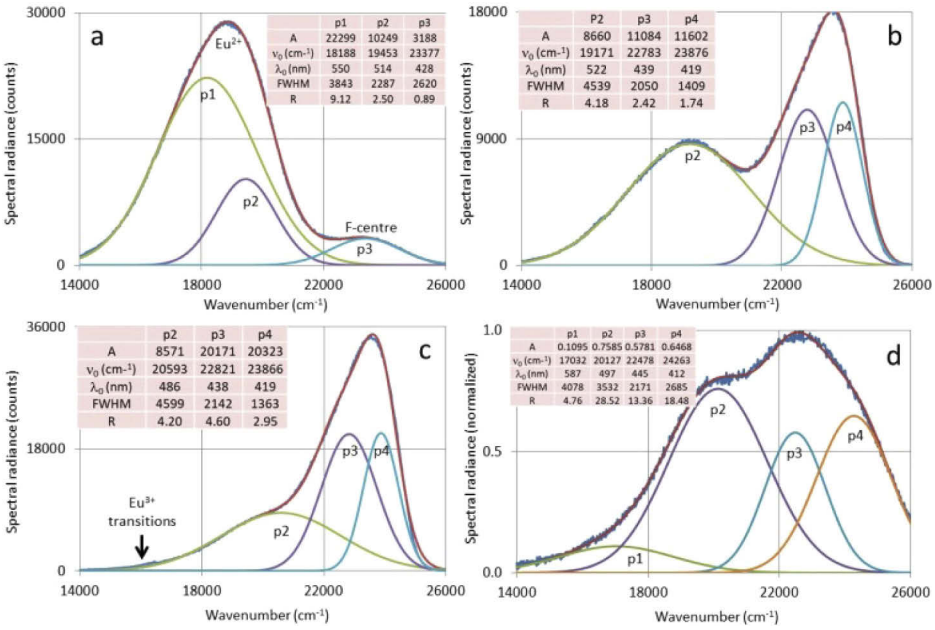

Fig. 9. (a): Deconvolution of spectrum 1 of Fig. 7 with 3 Gaussian profiles. (b): Deconvolution of spectrum 3 of Fig. 7 with 3 Gaussian profiles. (c): Deconvolution of spectrum 5 of Fig. 7 with 3 Gaussian profiles. (d): Deconvolution with 4 Gaussian profiles of CL spectrum of BA3 ($BaAl_2O_4$ with 500 ppm Eu) recorded at -170°C. The inserted Tables indicate the amplitude (A), the peak wavenumber (ν_0), peak wavelength (λ_0), full width at half maximum (FWHM) and the radiance (R, integrated intensity) of the profiles.

Optical Materials EXPRESS

is usually not observed at this condition in the presence of a Eu^{2+} dope. In the case of short e-beam exposure at -170°C (Fig. 9(a)), the p3 profile can be interpreted as F-centre emission. However, the p2 profile could consist of both Eu^{2+} emission and F-center emission. In that case the p1 is largely representing the Eu^{2+} emission, which indicates that this emission band is already largely referring to Eu^{2+} emission from $BaAl_2O_4$ in the paraelectric phase. Kawaguchi et al. [7] described the $P6_3 \rightarrow P6_322$ transition in hexagonal $BaAl_2O_4$ at room temperature after incorporating a small quantity Sr in the lattice. This was confirmed in our study of $Sr_{1-x}Ba_xAl_2O_4$ doped with Eu^{2+} [5]. It is interesting to see that the F-centre band in Figs. 7 and 9 is asymmetric and cannot be represented by a single Gaussian profile. At least two Gaussian profiles (p3 and p4) are needed for adequate representation. This could mean that the F-centres in $BaAl_2O_4$, which, in analogy with α-Al_2O_3, are related to oxygen vacancies, refer to (at least) two different oxygen sites. This explains the occurrence of the p3 and p4 profiles representing the F-centre bands in Figs. 3 and 9.

Figure 7 illustrates that the radiance of the F-centre band at 425 nm, being $R_{p3}+R_{p4}$, increases with the exposure time of the e-beam, while the radiance of the Eu^{2+} at about 500 nm decreases. This behaviour has been plotted in Fig. 10.

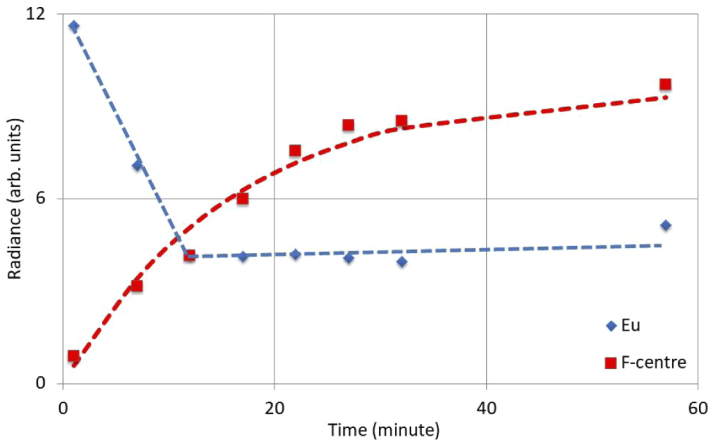

Fig. 10. F-centre and Eu^{2+} radiance of $Ba_{0.97}Eu_{0.03}Al_2O_4$ at -170°C versus time of e-beam exposure. The radiances have been calculated from the profiles after deconvolution of the spectra as illustrated in Fig. 9. The dashed curve that has been fitted through the F-centre points represents a first order reaction, whereas the dashed lines through the Eu points are guiding the eye.

Figure 10 indicates that the decrease of the Eu^{2+} emission band stopped after 12 minutes of e-beam exposure and then remained essentially constant upon continued e-beam exposure. From Fig. 10 it can be concluded that the increase of the F-centre radiance during e-beam exposure is not directly related to the decrease of the radiance of the Eu-band; however, a correspondence between the two processes cannot be denied. In section 4 we shall discuss the dashed curve, which represents a first order reaction for the increase of the F-centre radiance.

4. Discussion

In the preceding section we have presented new results of CL-measurements on $BaAl_2O_4$ doped with various quantities of Eu^{2+}. Before starting the discussion we shall summarize these results.

1. Undoped $BaAl_2O_4$ manifested intrinsic CL at 460 nm, which increased modestly at low temperature and did not change significantly upon exposure to the e-beam.

Optical Materials EXPRESS

2. Doping $BaAl_2O_4$ with Eu^{2+} changed the properties of the intrinsic luminescence band: it became more sensitive to temperature variations and the band manifested a blue shift.

3. E-beam exposure of $Ba_{0.97}Eu_{0.03}Al_2O_4$ at low temperature increased the intrinsic luminescence band strongly while the Eu^{2+} emission decreased by about 70%. The Eu^{2+} emission band became symmetric, indicating that $BaAl_2O_4$:Eu has changed to the $P6_322$ phase upon e-beam exposure at low temperature.

4. We have assigned this intrinsic band in $BaAl_2O_4$ to F-centre emission.

F-centres in α-Al_2O_3 are oxygen vacancies occupied by two electrons. These colour centres can be formed by bombardment with high energy particles (neutrons or electrons) or annealing Al_2O_3 at high temperature in a C crucible [41–43,45], which generates a reducing atmosphere. In the case of electron bombardment on α-Al_2O_3 it is assumed that a singly charged F^+ centre is converted to an F-centre by electron impact, while Makhov et al. [43] found upon exposing ruby crystals (α-Al_2O_3:Cr^{3+}) to 50 MeV electrons at room temperature that the F-centre luminescence band disappeared. This result indicates that the temperature and the presence of Cr are important parameters in the creation or annihilation of F-centres in Al_2O_3. Although we have detected Cr in our $BaAl_2O_4$ samples as mentioned above, the amount is assumed to be very small (<20 ppm) and its effect on the energy transfer in $BaAl_2O_4$ will therefore be neglected in the following considerations. In addition to the second point in the summary of the most important results presented above, it is worthwhile to mention that the F-centre luminescence in $BaAl_2O_4$ and $SrAl_2O_4$ behave differently. The undoped $BaAl_2O_4$ manifests clearly F-centre luminescence at room temperature, whereas in undoped $SrAl_2O_4$ the F-centre luminescence (excited by X-rays [32]) is quenched at room temperature. In the doped materials the behaviour is not so different: in both $BaAl_2O_4$:Eu^{2+} and $SrAl_2O_4$:Eu^{2+} the F-centre luminescence is quenched at room temperature. The latter information is from the work of Bierwagen et al. [28], where we have identified the 440 nm band with F-centre luminescence. More research will be necessary to understand these differences in quenching behaviour.

Figure 11 presents the most relevant energy levels of the F- and F^+-centres and a Eu^{2+} ion in $BaAl_2O_4$.

In Fig. 11 the Eu^{2+} $^8S_{7/2}$ ground state level and the lowest 5d level after relaxation have been indicated. After excitation to a higher Eu^{2+} 5d level, the Eu^{2+} ion relaxes radiationless to the $5d_1$ level (arrow 1a) from where the electron can relax to the ground state as indicated by the arrow 2. This arrow represents the 500 nm luminescence band of Eu^{2+} in $BaAl_2O_4$. Upon increasing the temperature thermal ionization according to arrow 3 becomes an alternative route: the electron can be dropped in the conduction band (CB) and the Eu^{2+} ion changes to Eu^{3+}. The electron may be caught/trapped eventually by an F^+-centre (arrow 8), to be discussed below. The difference between the bottom of the CB and the $5d_1$ level for $BaAl_2O_4$:Eu^{2+} is 0.4 eV, as indicated in the insert of Fig. 6. The barrier energy E_q in Fig. 6 can be explained either in terms of thermally activated cross-over from the Eu^{2+} 5d excited state to the 4f state or thermal ionization from the 5d state to the bottom of the conduction band, as shown in Fig. 11. Silver and Withnall [50] suggested that thermal ionization was the mechanism that quenched the luminescence in $Gd_3Al_5O_{12}$:Ce^{3+}, while Ueda et al. [29] have recently proved that this is also the quenching mechanism in $Y_3Al_5O_{12}$:Ce^{3+} (at rather high temperature). We assume that thermal ionization is also the quenching mechanism in $BaAl_2O_4$:Eu^{2+} and $SrAl_2O_4$:Eu^{2+} due to the similarity between the garnets and the aluminates. During e-beam exposure at low temperature the change of the shape of the Eu^{2+} emission band has been interpreted above as a phase change from the $P6_3$ to $P6_322$. We assume that energy difference between Eu^{2+} $4f^65d^1$ level and the bottom of the CB is smaller in the $P6_322$ phase of $BaAl_2O_4$ than in the $P6_3$ phase. This means that the alternative quenching route becomes more attractive from an energy point of view and, hence, it explains the loss of the Eu^{2+} radiance in Fig. 10.

Optical Materials EXPRESS

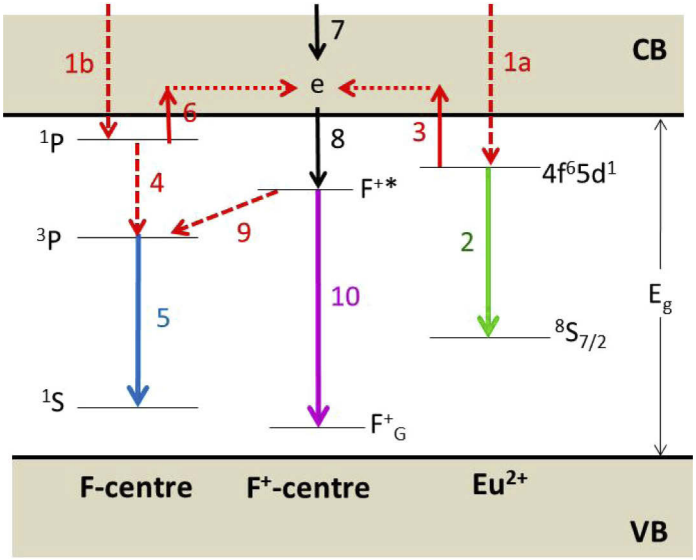

Fig. 11. Simplified energy diagram of Eu^{2+}, F-centre and F^+-centre in $BaAl_2O_4$. VB = valence band, CB = conduction band, E_g = band gap, F^+_G is ground level of F^+-centre, F^{+*} refers to a simplified (non-split) representation of excited states of F^+-centre. The arrows are explained in the text.

At the left hand side of Fig. 11 the positioning of the F- and F^+-centre levels in $BaAl_2O_4$ is presented. The location of these levels is (still) speculative, because we do not have enough data for a reliable positioning of them. As described by Lee and Crawford [45], an F -centre in Al_2O_3, and also in $BaAl_2O_4$, may be compared to a He atom, with a doubly charged virtual nucleus, the oxygen vacancy, and two electrons. The quasi He levels will be split according to the local symmetry conditions of the oxygen vacancy. For the present consideration we do not need this complication. Tentatively we position the ^{1}P level of the F-centre just below the bottom of the CB of $BaAl_2O_4$, as is done for the F- centre in Al_2O_3 [42,45,46]. The F^{+*}- level, which is represented in Fig. 11 as a non-split level, has been situated below the CB of α-Al_2O_3 at a distance >>kT as indicated by Evans et al. [46]. It is assumed that an identical positioning of this level applies in $BaAl_2O_4$. In other words, when the electron has been trapped by the F^+- centre, it cannot be promoted to the CB at room temperature. Upon excitation of the F-centre by the e-beam, the ^{1}P state is excited (arrow 1b), which can radiationless transfer to the ^{3}P level (arrow 4) and from there jump to the ^{1}S ground state, indicated by arrow 5. This latter transition is spin forbidden and it thus leads to a rather slow decay of the F- centre luminescence in α-Al_2O_3. When the temperature is increased, we envisage thermal ionization from the ^{1}P level to the CB as indicated by arrow 6. Since the ^{1}P level is assumed to be positioned rather close to the bottom of the CB (<0.4 eV), this thermal ionization takes place at much lower temperatures than the process indicated by arrow 3. When the electron enters the CB, it may diffuse to an F^+- centre and convert it to an F-centre as indicated in Eq. (2) and represented in Fig. 11 by arrow 8. This newly formed F- centre then relaxes to the ^{3}P level, indicated by arrow 9, and from there the excited electron may relax to the ground state while emitting light (arrow 5). Jonnard et al. [51] described the corresponding $F^+ \rightarrow F$ conversion in α-Al_2O_3 in detail. Their process 2b: $F+^* + e \rightarrow F^*$, where F^* is equivalent to the excited state ^{3}P of the F-centre, is in fact a combination of the arrows 8 and 9 in Fig. 11. De-excitation of the F^{+*}- state by emission of UV radiation is indicated by arrow 10: this radiation could not be observed with our spectrometer (as it was beyond its wavelength range). The process indicated by arrow 6 largely manifests the quenching

Optical Materials EXPRESS

of the F- centre luminescence and explains the increase in Fig. 4 of the 430 nm band of sample BA3 upon lowering the temperature, because the electron catching/trapping process indicated by arrow 8 is harvesting only a small part of the promoted electrons (arrow 6). Finally, the e-beam is also directly creating electron-hole pairs in the $BaAl_2O_4$ lattice. An electron created in this way may be first caught by an F^+- centre as shown by the arrows 7 and 8 and then it relaxes to the ^3P state of the F- centre as mentioned above (arrow 9). The processes indicated by the arrows 7, 8, 9 and 5 explain the luminescence of the 430 nm band in Fig. 7 and are quantitatively described by Eq. (4), to be discussed hereafter. By e-bombarding the concentration of F^+- centres is diminishing, whereas the concentration of F- centres increases. The consequence of this model is thus that the luminescence from the F^+- centre is decreasing upon exposure to a high-energy e-beam. A decrease of the F^+- centre emission was actually observed by Caulfield et al. [52] upon bombarding α-Al_2O_3 with high energy electrons. In Fig. 11 we have not indicated the direct formation of F- centres by the e-beam, neither did we indicate the direct excitation of an F^+- centre by the e-beam. Based on the work on neutron bombardment of α-Al_2O_3, such a process is thought to be feasible. However, based on the model presented above and the literature data of α-Al_2O_3, we conclude that by e-beam exposure in TEM-mode the strong increase of the F- centre emission at 430 nm as depicted in Fig. 7 is primarily due to exhausting the F^+-centres and relaxation of the neutralised F^+- centres via arrow 9. If the preceding model about the F-centre luminescence is realistic for $BaAl_2O_4$ with 3% Eu^{2+}, then the question is why we have not observed similar phenomena in undoped $BaAl_2O_4$ or $BaAl_2O_4$ with 500 ppm Eu. We assume that the phase transition from the ferroelectric $P6_3$ phase to the $P6_322$ phase is explaining this difference. Not only exposure to an e-beam is triggering this phase transition, but also incorporation of a small quantity of Sr^{2+} into $BaAl_2O_4$ [5,7]. Since the sizes of the Eu^{2+} and Sr^{2+} ions are similar, we assume that $Ba_{0.97}Eu_{0.03}Al_2O_4$ is easier to transfer to the $P6_322$ phase than $BaAl_2O_4$. If this is the case, then the same arguments may be applied as above: the thermal ionization of Eu^{2+} is increased and more electrons are transferred from the Eu^{2+} $4f^65d^1$ level to the CB. This will increase the concentration of F^+ centres by electron trapping via arrow 8.

Finally, we shall introduce a simple quantitative analysis of the increase of the radiance of the F-centre emission upon e-beam exposure as illustrated in Fig. 7. Let us assume that (R_{p3}+R_{p4}) as shown in Figs. 9(b) and 9(c) is proportional to the number of the F-centres that are responsible for the luminescence of p3 and p4. This number per unit of volume will be indicated by N_F, which changes upon e-beam exposure. It is supposed that N_F is related to a fixed number of defects indicated by N_u, which is larger than the actual value of N_F. In the framework of the F-centre hypothesis, it is obvious to identify N_u with the number of F^+ centres and the basic reaction taking place upon bombarding $BaAl_2O_4$ crystals with electrons would be:

$$F^+ + e^- \rightarrow F. \tag{2}$$

This reaction represents the neutralisation of F^+ centers by electrons. Because of the limited wavelength range of the Gatan spectrometer, we could not simultaneously record the F^+ luminescence, which is expected to be at ~335 nm [41], with the spectra shown in Fig. 7. Due to this we leave N_u unassigned. By assuming a first order reaction by e-beam exposure as indicated by Eq. (2), the following equation can be written,

$$\frac{dN_F}{dt} = k(N_u - N_F), \tag{3}$$

where k is the rate constant, which is primarily dependent on the current density of the e-beam. By solving Eq. (3) it appears that

$$N_F = N_u(1 - e^{-kt}) \propto (R_{p3} + R_{p4}). \tag{4}$$

By fitting Eq. (4) to the data points in Fig. 10, k was found to be 0.063 $minute^{-1}$. Figure 10 shows that full conversion of F^+ to F took more than one hour at a current density of ≈7 mA/cm^2

Optical Materials EXPRESS

and electron energy of 200 keV. The behaviour of $R_{p3}+R_{p4}$ in the reverse direction could not be determined because of hysteresis. By warming up the sample, the transition to the original situation before e-beam exposure occurred rather "suddenly".

The explanation above on the origin of the 430 nm band in $BaAl_2O_4:Eu^{2+}$ is an important building block for its mixed luminescence: intrinsic lattice luminescence (F- centre) and Eu^{2+} luminescence. This type of mixed luminescence has been described by us in an earlier study on $Y_2O_3:Ln^{3+}$ (Ln = Eu, Tb, Tm and Er) [53,54].

As we discussed, the F centre emission is rather slow and relatively few electrons are involved. This may be concluded from the work described here as there is little evidence for Eu^{3+} in the figures, although some is apparent in Fig. 9(c). Finally, the fact that the F centres are not observed in the PL spectra shows that the excitation energies used for generating the PL spectra are not able to ionise the Eu^{2+} cations. In a follow-up work we shall report Raman spectra of $BaAl_2O_4$, which will provide more evidence in support of the scheme we put forward in Fig. 11 [38].

5. Conclusions

The study presented in this paper focusses on the properties of the intrinsic emission of undoped $BaAl_2O_4$ and the 425 nm luminescence band of $Ba_{0.97}Eu_{0.03}Al_2O_4$. The results have allowed us to propose a new hypothesis about the origin of the emission (side) band at 425 nm in the PL and CL spectra of $BaAl_2O_4:Eu^{2+}$. This new hypothesis refers to the luminescence of F-centres coexisting besides the regular emission of the Eu^{2+} ion in $BaAl_2O_4$. The most interesting results found in this study were the strong increase of the F-centre emission of $BaAl_2O_4$ upon exposure to an e-beam at low temperature, while at the same time the Eu^{2+} emission band at about 500 nm decreased. Both phenomena have been explained by assuming that $BaAl_2O_4$ experienced a transition from the ferroelectric $P6_3$ phase to the paraelectric $P6_322$ phase. The thermal quenching of the 500 nm PL of $BaAl_2O_4:Eu^{2+}$ at about 140°C has been explained in terms of thermal ionization of Eu^{2+}.

It is not surprising that the unravelling of the F- centre emission from $BaAl_2O_4$ and the Eu^{2+} -related emission from $BaAl_2O_4:Eu^{2+}$ was not proposed earlier, because their emission bands largely overlap. However, we hope that the results described in this article herald the start of more research about the F- centre hypothesis. One of the first questions that must be addressed is the identification of the luminescence of the F^+- centre in undoped $BaAl_2O_4$ that is expected to be at about 335 nm. Another question is the nature/origin of is the luminescence of the emission band at about 520 nm: may it be assigned to an F_2-centre? Finally the conclusions presented here are a step forward in the understanding of how the phosphor lattice (in this case based on AlO_4 tetrahedra) affects the emission properties of the final phosphor of which it forms part.

Funding

Engineering and Physical Sciences Research Council (CONVERTED (JeS no. TS/1003053/1), FAB3D, PRISM (EP/N508974/1), PURPOSE (TP11/MFE/6/1/AA129F; EP-SRC TS/G000271/1)); TECHNOLOGY STRATEGY BOARD (CONVERT).

Acknowledgments

We are grateful to the EPSRC and Technology Strategy Board (TSB) for funding the PURPOSE (TP11/MFE/6/1/AA129F; EP-SRC TS/G000271/1) and CONVERTED (JeS no. TS/1003053/1), PRISM (EP/N508974/1) and FAB3D programs. We are finally grateful to the TSB for funding the CONVERT program.

References

1. J. Silver, G. Fern, and R. Withnall, "Color Conversion Phosphors for Light Emitting Diodes," In *Materials for Solid State Lighting and Displays*. A. Kitai, ed. Wiley Inc., New York (2017), pp. 91–134.

Optical Materials EXPRESS

2. R. Stone, "An investigation into novel red emitting phosphors and their applications", Thesis, Brunel University, London (UK), (2011).
3. J. Silver, G. Fern, and R. Withnall (the late), "Chemistry and Synthesis of Inorganic Light-Emitting Phosphors", In *Handbook of Visual Display Technology*, (2015), pp. 1–13.
4. L. Yu, D. den Engelsen, J. Gorobez, G. R. Fern, T. G. Ireland, C. Frampton, and J. Silver, "Crystal structure, photoluminescence and cathodoluminescence of $Sr_{1-x}Ca_xAl_2O_4$ doped with Eu^{2+}," Opt. Mater. Express **9**(5), 2175–2195 (2019).
5. M. Volhard, L. Yu, D. den Engelsen, G. Fern, T. Ireland, and J. Silver, "Crystal structure, photoluminescence and cathodoluminescence of $Sr_{1-x}Ba_xAl_2O_4$ doped with Eu^{2+}," *Opt. Mater. Express*, in press.
6. M. Volhard, D. den Engelsen, G. Fern, T. Ireland, and J. Silver, "Crystal structure, photoluminescence and cathodoluminescence of $Ba_{x-1}Ca_xAl_2O_4$ doped with Eu^{2+}," Opt. Mater. Express **9**(10), 3895–3910 (2019).
7. S. Kawaguchi, Y. Ishii, E. Tanaka, H. Tsukasaki, Y. Kubota, and S. Mori, "Giant thermal vibrations in the framework compounds $Ba_{1-x}Sr_xAl_2O_4$," Phys. Rev. B **94**(5), 054117 (2016).
8. S. Y. Huang, R. Von Der Mühll, J. Ravez, and M. Couzi, "Phase transition and symmetry in $BaAl_2O_4$," Ferroelectrics **159**(1), 127–132 (1994).
9. S. Y. Huang, R. Von Der Mühll, J. Ravez, J. P. Chaminade, P. Hagenmuller, and M. Couzi, "A propos de la ferroélectricité dans $BaAl_2O_4$," J. Solid State Chem. **109**(1), 97–105 (1994).
10. A. M. Abakumov, O. I. Lebedev, L. Nistor, G. Van Tendeloo, and S. Amelinkx, "The ferroelectric phase transition in tridymite type $BaAl_2O_4$ studied by electron microscopy," Phase Transitions **71**(2), 143–160 (2000).
11. U. Rodehorst, M. A. Carpenter, S. Marion, and C. M. Henderson, "Structural phase transitions and mixing behaviour of the Ba-aluminate ($BaAl_2O_4$)-Sr-aluminate ($SrAl_2O_4$) solid solution," Mineral. Mag. **67**(5), 989–1013 (2003).
12. J. Kaur, B. Jaykumar, V. Dubey, R. Shrivastava, and N. S. Suryanarayana, "Optical properties of rare Earth-doped barium aluminate synthesized by different methods – A Review," Res. Chem. Intermed. **41**(4), 2317–2343 (2015).
13. A.-K. Larsson, R. L. Withers, J. M. Perez-Mato, J. D. Fitz Gerald, P. J. Saines, B. J. Kennedy, and Y. Liu, "On the microstructure and symmetry of apparently hexagonal $BaAl_2O_4$," J. Solid State Chem. **181**(8), 1816–1823 (2008).
14. G. Blasse and A. Bril, "Fluorescence of Eu^{2+}-activated alkaline-earth aluminates," Philips Res. Rep. **23**, 201–206 (1968).
15. S. H. M. Poort, W. P. Blokpoel, and G. Blasse, "Luminescence of Eu^{2+} in Barium and Strontium Aluminate and Gallate," Chem. Mater. **7**(8), 1547–1551 (1995).
16. M. Peng and G. Hong, "Reduction of Eu^{3+} to Eu^{2+} in $BaAl_2O_4$ phosphor prepared in an oxidizing atmosphere and luminescent properties of $BaAl_2O_4$:Eu," J. Lumin. **127**(2), 735–740 (2007).
17. B. M. Mothudi, O. M. Ntwaeaborwa, J. R. Botha, and H. C. Swart, "Photoluminescence and phosphorescence properties of MAl_2O_4:Eu^{2+}, Dy^{3+} (M = Ca, Ba, Sr) phosphors prepared at an initiating combustion temperature of 500°C," Phys. B **404**(22), 4440–4444 (2009).
18. B. P. Kore, N. S. Doble, and S. J. Doble, "Study of anomalous emission and irradiation effect on the thermoluminescence properties of barium aluminate," J. Lumin. **150**, 59–67 (2014).
19. R. Stefani, L. C. V. Rodrigues, C. A. A. Carvalho, M. C. F. C. Felinto, H. F. Brito, M. Lastusaari, and J. Hölsä, "Persistent luminescence of Eu^{2+} and Dy^{3+} doped barium aluminate ($BaAl_2O_4$:Eu^{2+},Dy^{3+}) materials," Opt. Mater. **31**(12), 1815–1818 (2009).
20. Q. He, G. Qiu, X. Xu, J. Qiu, and X. Yu, "Photostimulated luminescence properties of Eu^{2+}-doped barium aluminate phosphor," Luminescence **30**(2), 235–239 (2015).
21. S. H. Ju, U. S. Oh, J. C. Choi, H. L. Park, T. W. Kim, and C. D. Kim, "Tunable color emission and solid solubility limit in $Ba_{1-x}Ca_xAl_2O_4$:$Eu_{0.001}{}^{2+}$ phosphors through the mixed states of $CaAl_2O_4$ and $BaAl_2O_4$," Mater. Res. Bull. **35**(11), 1831–1835 (2000).
22. H. F. Brito, M. C. F. C. Felinto, J. Hölsä, T. Laamanen, M. Lastusaari, M. Malkamäki, P. Novák, L. C. V. Rodrigues, and R. Stefani, "DFT and synchrotron radiation study of Eu^{2+} doped $BaAl_2O_4$," Opt. Mater. Express **2**(4), 420–431 (2012).
23. F. C. Palilla, A. K. Levine, and M. R. Tomkus, "Fluorescent Properties of Alkaline Earth Aluminates of the Type MAl_2O_4 Activated by Divalent Europium," J. Electrochem. Soc. **115**(6), 642–644 (1968).
24. J. Botterman, J. Joos, and P. F. Smet, "Trapping and detrapping in $SrAl_2O_4$:Eu,Dy persistent phosphors: Influence of excitation wavelength and temperature," Phys. Rev. B: Condens. Matter Mater. Phys. **90**(8), 085147 (2014).
25. J. M. Ngaruiya, S. Nieuwoudt, O. M. Ntwaeaborwa, J. J. Terblans, and H. C. Swart, "Resolution of Eu^{2+} asymmetrical emission peak of $SrAl_2O_4$:Eu^{2+}, Dy^{3+} phosphor by cathodoluminescence measurements," Mater. Lett. **62**(17-18), 3192–3194 (2008).
26. D. Dutczak, T. Jüstel, C. Ronda, and A. Meijerink, "Eu^{2+} luminescence in strontium aluminates," Phys. Chem. Chem. Phys. **17**(23), 15236–15249 (2015).
27. F. Clabau, X. Rocquefelte, S. Jobic, P. Deniard, M.-H. Whangbo, A. Garcia, and T. Le Mercier, "Mechanism of phosphorescence appropriate for the long-lasting phosphors Eu^{2+}-doped $SrAl_2O_4$ with codopants Dy^{3+} and B^{3+}," Chem. Mater. **17**(15), 3904–3912 (2005).
28. J. Bierwagen, S. Yoon, N. Gartmann, B. Walfort, and H. Hagemann, "Thermal and concentration dependent energy transfer of Eu^{2+} in $SrAl_2O_4$," Opt. Mater. Express **6**(3), 793–803 (2016).
29. J. Ueda, T. Nakanishi, Y. Katayama, and S. Tanabe, "Optical and optoelectronic analysis of persistent luminescence in Eu^{2+}-Dy^{3+} codoped $SrAl_2O_4$ ceramic phosphor," Phys. Status Solidi C **9**(12), 2322–2325 (2012).

Optical Materials EXPRESS

30. L. Ning, X. Huang, Y. Huang, and P. A. Tanner, "Origin of Green Persistent Luminescence of Eu-Doped $SrAl_2O_4$ from Multiconfigurational *Ab Initio* Study of $4f^7 \rightarrow 4f^6 5d^1$ Transitions," J. Mater. Chem. C **6**(25), 6637–6640 (2018).
31. M. Nazarov, M. G. Brik, D. Spassky, B. Tsukerblat, A. Nor Nazida, and M. N. Ahmad-Fauzi, "Structural and electronic properties of $SrAl_2O_4$:Eu^{2+} from density functional theory calculations," J. Alloys Compd. **573**(1), 6–10 (2013).
32. V. Vitola, D. Millers, K. Smits, I. Bite, and A. Zolotarjovs, "The search for defects in undoped $SrAl_2O_4$ material," Opt. Mater. **87**, 48–52 (2019).
33. L. Zhang, L. Wang, and Y. Zhu, "Synthesis and Performance of $BaAl_2O_4$ with a Wide Spectral Range of Optical Absorption," Adv. Funct. Mater. **17**(18), 3781–3790 (2007).
34. A. Pandey and M. L. Chithambo, "Thermoluminescence of persistent-luminescence phosphor, $BaAl_2O_4$; A stuffed tridymite," Radiat. Meas. **120**(1), 73–77 (2018).
35. S. Benourdja, ÜH Kaynar, M. Ayvacikli, Y. Karabulut, J. Garcia Guinea, A. Canimoglu, L. Chahed, and N. Can, "Preparation and cathodoluminescence characteristics of rare earth activated $BaAl_2O_4$ phosphors," Appl. Radiat. Isot. **139**, 34–39 (2018).
36. M. Ayvacikli, "Characterization of a Green-Emitting Copper-Doped Barium Aluminate Phosphor," Spectrosc. Lett. **47**(7), 504–511 (2014).
37. N. Suriyamurthy and B. S. Panigrahi, "Luminescence of $BaAl_2O_4$: Mn^{2+}, Ce^{3+} phosphors," J. Lumin. **127**(2), 483–488 (2007).
38. D. den Engelsen, G. R. Fern, T. Ireland, and J. Silver, "Laser-activated luminescence of $BaAl_2O_4$:Eu", ECS J. Solid State Sci. Technol., submitted.
39. A. I. Surdo, V. S. Kortov, and V. A. Pustovarov, "Luminescence of F and F^+ centers in corundum upon excitation in the interval from 4 to 40 eV," Radiat. Meas. **33**(5), 587–591 (2001).
40. J. Valbis and N. Itoh, "Electronic excitations, luminescence and lattice defect formation in α-Al_2O_3 crystals," Radiat. Eff. Defects Solids **116**(1-2), 171–189 (1991).
41. M. Itou, A. Fujivara, and T. Uchino, "Reversible photoinduced interconversion of color centers in α - Al_2O_3 prepared under vacuum," J. Phys. Chem. C **113**(49), 20949–20957 (2009).
42. B. G. Draeger and G. P. Summers, "Defects in unirradiated α-Al_2O_3," Phys. Rev. B **19**(2), 1172–1177 (1979).
43. V. N. Makhov, A. Lushchik, C. B. Lushchik, M. Kirm, E. Vasil'chenko, S. Vielhauer, V. V. Harutunyan, and E. Aleksanyan, "Luminescence and radiation defects in electron-irradiated Al_2O_3 and Al_2O_3:Cr," Nucl. Instrum. Methods Phys. Res., Sect. B **266**(12-13), 2949–2952 (2008).
44. Y. Zorenko, T. Zorenko, T. Voznyak, A. Mandowski, Q. Xia, M. Batentschuk, and J. Friedrich, "Luminescence of F^+ and F centers in Al_2O_3-Y_2O_3 oxide compounds," IOP Conf. Ser.: Mater. Sci. Eng. **15**, 012060 (2010).
45. K. H. Lee and J. H. Crawford Jr., "Luminescence of the F center in sapphire," Phys. Rev. B **19**(6), 3217–3221 (1979).
46. B. D. Evans, G. J. Pogatshnik, and Y. Chen, "Optical properties of lattice defects in α-Al_2O_3," Nucl. Instrum. Methods Phys. Res., Sect. B **91**(1-4), 258–262 (1994).
47. W. Hörkner and H. K. Müller-Buschbaum, "Zur Kristallstruktur von $BaAl_2O_4$," Z. Anorg. Allg. Chem. **451**(1), 40–44 (1979).
48. S. Lizzo, E. P. Klein Nagelvoort, R. Erens, A. Meijerink, and G. Blasse, "On the quenching of the Yb^{2+} luminescence in different host lattices," J. Phys. Chem. Solids **58**(6), 963–968 (1997).
49. D. den Engelsen, G. R. Fern, T. G. Ireland, and J. Silver, "Reassignment of electronic transitions in the laser-activated spectrum of nanocrystalline Y_2O_3:Er^{3+}," J. Lumin. **196**, 337–346 (2018).
50. J. Silver and R. Withnall, "Color Conversion Phosphors for LEDS," in "*Luminescent Materials and Applications*", Ed. A. Kitai, 2008, Wiley, Chichester, pp92.
51. P. Jonnard, C. Bonnelle, G. Blaise, G. Rémond, and C. Roques-Carmes, "F^+ and F centers in α-Al_2O_3 by electron-induced x-ray emission spectroscopy and cathodoluminescence," J. Appl. Phys. **88**(11), 6413–6417 (2000).
52. K. J. Caulfield, R. Cooper, and J. F. Boas, "Luminescence from electron-irradiated sapphire," Phys. Rev. B **47**(1), 55–61 (1993).
53. D. den Engelsen, G. R. Fern, T. G. Ireland, P. G. Harris, P. R. Hobson, A. Lipman, R. Dhillon, P. J. Marsh, and J. Silver, "Ultraviolet and blue cathodoluminescence from cubic Y_2O_3 and Y_2O_3:Eu^{3+} generated in a transmission electron microscope," J. Mater. Chem. C **4**(29), 7026–7034 (2016).
54. D. den Engelsen, G. R. Fern, T. G. Ireland, and J. Silver, "Cathodoluminescence of Y_2O_3:Ln^{3+} (Ln = Tb, Er and Tm) and Y_2O_3:Bi^{3+} nanocrystalline particles at 200 keV," RSC Adv. **8**(1), 396–405 (2018).